

## P5.15 LEE WAVES OVER COMPLEX TOPOGRAPHY DURING MAP

James D. Doyle<sup>1</sup>, Ronald B. Smith<sup>2</sup>, and Gregory S. Poulos<sup>3</sup>

<sup>1</sup>Naval Research Laboratory, Monterey, CA

<sup>2</sup>Yale University, New Haven, CT

<sup>3</sup>Colorado Research Associates, Boulder, CO

### 1. INTRODUCTION

As stably stratified air flows over a topographic barrier, internal mountain waves are generated. Linear theory suggests that the nature of the mountain wave response is determined by the mountain shape and size, as well as the Scorer parameter,

$$l^2 = \frac{N^2}{U^2} - \frac{1}{U} \frac{\partial^2 U}{\partial z^2}, \quad (1)$$

where  $N$  is the Brunt-Väisälä frequency, and  $U$  is the mean cross mountain wind speed. When  $l^2$  decreases rapidly with height resonant waves can develop such that these standing gravity waves, or trapped lee waves, have a periodic character with respect to their vertical structure near the ground. Lee waves have been the subject of numerous studies for more than 50 years. Recent measurements from the Mesoscale Alpine Programme (MAP) and subsequent numerical modeling results suggest that processes that have received relatively little emphasis previously, such as boundary layer (e.g., Smith et al. 2001) and moist effects, may be important for lee wave generation and evolution.

A series of quasi-periodic mountain waves were observed in the lee of Grossglockner in the eastern Alps by the National Center for Atmospheric Research (NCAR) Electra research aircraft equipped with a suite of instrumentation including downlooking Scanning Aerosol Backscatter Lidar (SABL) and Global Positioning System (GPS) dropsondes during MAP IOP 2 on 20 September 1999. The Hohe Tauern is a quasi-two-dimensional, east-west oriented range that includes the highest peak in Austria, Grossglockner at 3797 m. The lee wave activity was observed during an extended period of deep-south foehn and was particularly intense on this day with a surface wind speed maximum of  $50 \text{ m s}^{-1}$  observed at Patscherkofel, near Innsbruck. Precipitation was observed upstream of the crest during the lee wave formation. It is noteworthy that in this case and a number of other situations during MAP, real-time mesoscale models forecasted vertically propagating large-amplitude waves rather than quasi-periodic partially trapped waves in the lee, as was often observed.

### 2. RESEARCH AIRCRAFT OBSERVATIONS

The Electra flight track consisted of a repeated series of six north-south oriented segments over Grossglockner at altitudes in the 4900-6700 m range, as shown in Fig. 1. The maximum vertical velocity measured was  $> 8 \text{ m s}^{-1}$  with a corresponding potential temperature perturbation  $> 10 \text{ K}$  at 4900 m. A total of 4-7

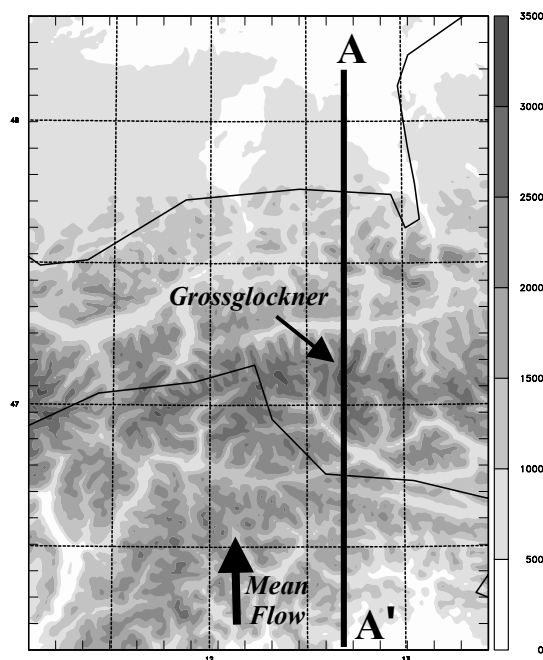


Fig. 1. The Electra flight track (AA') and topography (m) of the Hohe Tauern region (shaded).

lee waves with a wavelength of 10-13 km were consistently measured. The shorter wavelength and smaller amplitude waves were observed downstream of the most significant mountain waves. The cross-mountain wind component at flight level ranged  $10\text{-}28 \text{ m s}^{-1}$ , with the strongest winds immediately in the lee of Grossglockner at 4900 m and weakest upstream of the Alpine crest. The backscatter coefficient from the downlooking SABL for the third flight segment, shown in Fig. 2, indicates a clear signature  $> 5$  lee waves and in agreement with the vertical parcel displacements computed using the Electra flight-level data. The most intense backscatter is apparently due to cloud liquid water in the wave crests, which were visually confirmed by the onboard scientists. The largest amplitude lee wave signature is located immediately downstream of the Alpine crest and suggests vertical parcel displacements of  $\sim 1.0 \text{ km}$ . It is noteworthy that the waves are not in optimal phase with the topographic features beyond the highest peak suggesting that the lower portion of a wave duct may reside above the surface in the boundary layer.

### 3. NUMERICAL SIMULATIONS

Numerical simulations were conducted with the NRL COAMPS nonhydrostatic modeling system (Hodur 1997) using four nested grids telescoping down to

*Corresponding Author Address:* James D. Doyle, Naval Research Laboratory, 7 Grace Hopper Ave., Monterey, CA 93943-5502; *e-mail:* doyle@nrlmry.navy.mil

the finest mesh with a horizontal grid increment of 1 km and 55 vertical levels. The model includes a full suite of physical parameterizations. The simulation for 1400 UTC 20 September 1999 (14 h), shown in Fig. 3, indicates a deep layer of large static stability, extending from the surface to 7 km, that is capped by a weak stability region, which extends upward to the tropopause at 10.5 km. Model sensitivity tests suggest that this weak stability layer forms due to latent heat release associated with precipitation upstream of the crest. Diagnostic calculations indicate a rapid decrease of  $\bar{\rho}^2$  with height, which is conducive for wave trapping, as a result of large low-level vertical shear and the weak stability aloft. The simulated lee waves are characterized by wavelengths of 10–15 km, vertical velocities  $>10 \text{ m s}^{-1}$ , potential temperature perturbations  $>8 \text{ K}$ , and isentropic vertical displacements  $\sim 1.0 \text{ km}$ , which are in reasonable agreement with the research aircraft observations. The simulation suggests that some mountain wave energy leaks through the duct and leads to amplifying waves in the lower stratosphere, in a layer of large vertical shear.

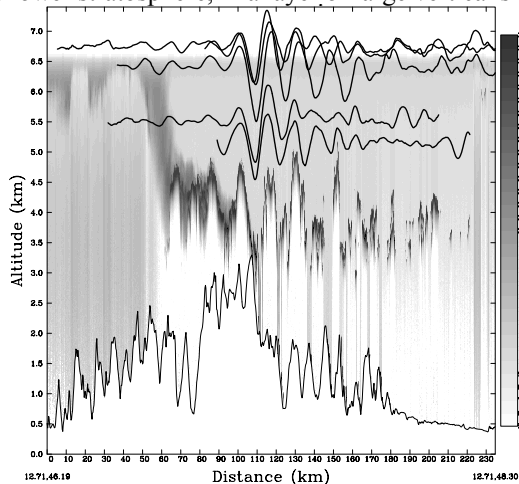


Fig. 2. The downlooking SABL backscatter coefficient and vertical parcel displacements from the Electra.

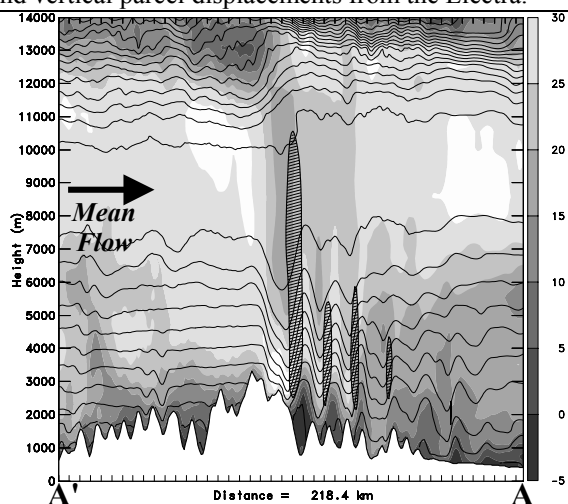


Fig. 3. COAMPS simulated cross-mountain (v) wind component (shaded,  $\text{m s}^{-1}$ ) and potential temperature (every 3 K) for 1400 UTC 20 September (14 h). The vertical velocity in excess of  $4 \text{ m s}^{-1}$  is hatched.

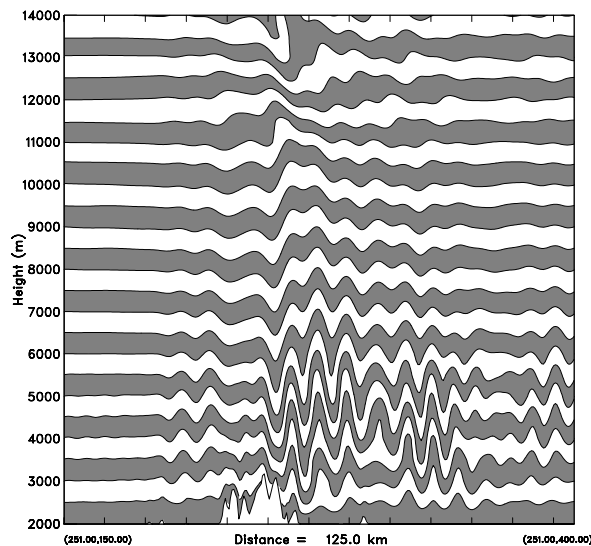


Fig. 4. Vertical displacement field from nonhydrostatic linear theory.

Blocking and boundary-layer processes upstream of the Alpine crest reduce the effective mountain height (Fig. 3) similar to that found by Smith et al. (2001). Composites of radiosonde and GPS dropsonde data confirm that an upstream blocked layer was present up to  $\sim 2 \text{ km}$ .

Simulations performed using a nonhydrostatic linear model (Smith et al. 2001), shown in Fig. 4, indicate that linear theory accurately represents the lee wavelength, but underestimates the wave amplitude by up to a factor of two. This result was confirmed by COAMPS linear simulations and agrees with previous studies (e.g., Smith 1976; Durran and Klemp 1982).

#### 4. FUTURE DIRECTIONS

A number of questions are unresolved for cases of lee waves generation over complex orography such as occurred during MAP IOP 2. The primary research issues include the: i) role of the upstream moist processes in modifying the ambient static stability, ii) upstream and downstream boundary layer effects, iii) characterization of the gravity wave breaking aloft, and iv) failure of real-time models in a number of lee wave cases during MAP. Our ongoing research will continue to apply the nonlinear and linear models, and analyze research aircraft data to explore these issues further.

#### ACKNOWLEDGEMENTS

The first author's research was supported by ONR PE-0601153N. Computing time was supported by a grant of HPC time from the DoD MSRC, Stennis, MS, and performed on a Cray T-90.

#### REFERENCES

- Durran, D.R., and J.B. Klemp, 1982: The effects of moisture on trapped mountain lee waves. *J. Atmos. Sci.*, **39**, 2490–2506.
- Hodur, R.M., 1997: The Naval Research Laboratory's Coupled Ocean/Atmosphere Mesoscale Prediction System (COAMPS). *Mon. Wea. Rev.*, **125**, 1414–1430.
- Smith, R.B., 1976: The generation of lee waves by the Blue Ridge. *J. Atmos. Sci.*, **33**, 507–519.
- Smith, R.B., S. Skubis, J.D. Doyle, A.S. Broad, C. Kiemle, H. Volkert, 2001: Gravity waves over Mt. Blanc. Submitted *J. Atmos. Sci.*